RESEARCH ON THE MECHANISM AND PRACTICE OF FRACTURE INITIATION DURING HYDRAULIC FRACTURING IN HARD ROOFS OF COAL MINE

by

Qigen DENG[a,b,c*], Yanjie YANG[a], Fajun ZHAO[a,b], and Yinsheng DU[a]

[a] School of Safety Science and Engineering, Henan Polytechnic University, Jiaozuo, China
[b] State Key Laboratory Cultivation Base for Gas Geology and Gas Control, Henan Polytechnic University, Jiaozuo, China
[c] Collaborative Innovation Center of Coal Work Safety and Clean High Efficiency Utilization, Jiaozuo, China

Original scientific paper
https://doi.org/10.2298/TSCI2303827D

A hydraulic fracture extension model was established, an extension criterion and an extension mode of hydraulic fracture were analyzed, and the theoretical prediction was compared with the practical results, a good agreement was observed. Furthermore, the direction of hydraulic fracture extension was also discussed, the results showed that the hydraulic fracture propagates from the cut to the bedding plane, forming a complex mixture of longitudinal and transverse fractures fracture network. The hydraulic fracture extension direction is influenced by its extension critical pressure and its extension pressure in the rock formation. Practice shows that hydraulic fracturing can effectively weaken the strength and integrity of the roof, so that the roof in the mining area can collapse in layers and stages. The present theoretical analysis can be used for reducing or eliminating the hazard of the hard roof to the working faces.

Key words: *extended guidelines, fracture propagation, fracturing fracture, effectiveness testing, fractal*

Introduction

The coal seams in China have complex conditions with about 1/3 of the coal seams having hard roofs [1]. A hard roof has high strength, and its collapse always sees no development of joint fissures. The roof is easy to cause a large area of overhanging roof after coal seam mining, especially the overhanging roof area is larger in the early stopping. The sudden collapse of large overhanging roof is easy to cause large impact damage to the bracket, deformation of the roadway surrounding rock, destabilization of the support structure, furthermore it can squeeze instantly the harmful gas out of the mining area, causing many safety problems [2, 3]. At present, the theory and technology to control the hard roofs mainly includes cumulative blasting, water injection softening and hydraulic fracturing. Injection of water to soften the rock layers requires the roof rock water absorption, so it does not work well. Blasting technology is rarely used in China because of its large volume of work, high cost, pollution of the underground air and the potential for vibration to cause safety hazards in and around the mines. Hydraulic fracturing technology was initially applied in the oil

* Corresponding author, e-mail: dengqigen@hpu.edu.cn

mining, and its practice in the coal mining has proved to be successful and effective in the initial caving, control of the surrounding rock of the roadway, and prevention of impact ground pressure [4-6].

In this study, the 1306 working face of No. 3 coal seam of a mine in Jincheng, Shanxi, China is used as the engineering background. The average depth of burial of the coal seam is 440 m, with an average thickness of 6.4 m and the dip angle is 1~3°. The main roof of the coal seam is dominated by medium-grained sandstone with a thickness of 6.3 m, which is medium-hard rock. The immediate roof is 4.2 m thick, mostly sandy mudstone, partially mudstone and siltstone, and the fissures are not developed, which is weak rock. The geostress level belongs to the low zone, which is dominated by tectonic stress.

Considering the practical engineering environment, this paper discusses the use of retreating hydraulic fracturing technology for control management of the hard and difficult to collapse roof, and water is acted as the expansion medium.

Hydraulic fracturing techniques and propagation theory

Directional hydraulic fracturing technology

The essence of directional hydraulic fracturing is to prefabricate a row of transverse grooves in the drilled fracturing section of the roof with a special drill bit in front of working face. High pressure water is injected into the drilled fracturing section, causes a concentration of tensile stresses at the tip of the groove and preferential cracking, resulting in a series of cracks in the hard rock along the bedding plane [1, 7], as illustrated in fig. 1.

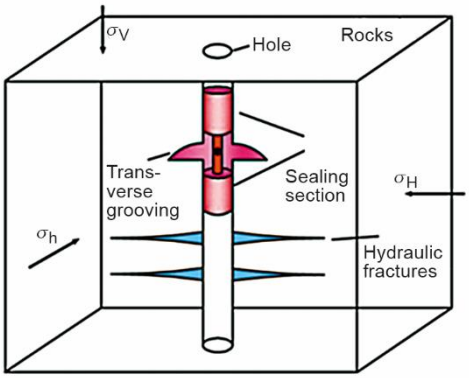

Figure 1. Diagram of directional hydraulic fracturing; *σ_V is the vertical stress, σ_H – the maximum horizontal principal stress, and σ_h – the minimum horizontal principal stress*

Through hydraulic fracturing, we can change the hard-to-collapse roof to the easy-to-collapse one, and the fractured overhanging roof ruptures and slides down to the mining area, which fully contacts with the gangue and broken coal, so the span of the cantilever beams of the curved triangular plates on both sides of the working face can be reduced, and the mining stress can not transfer to the cutting eye and the roadway [8]. The change of the roof before and after using directional hydraulic fracturing is shown in fig. 2.

Mechanisms of fracture initiation during hydraulic fracturing

Hydraulic fracturing can be seen as a Penny-shaped fracture model [9-11]. Figure 3 shows a hydraulic fracture in a rock medium that is expanding. The *y*-axis is a schematic diagram of the fracturing borehole, and the rest of fig. 3 shows a fracture unit, and the unit is filled with high pressure fluid (blue). Under the action of hydraulic pressure, different parts of the fracture unit have different responses: the blue part indicates the area that has been ruptured, and the shaded area in front of the fracture tip is the rupture process area which is about to rupture [12, 13].

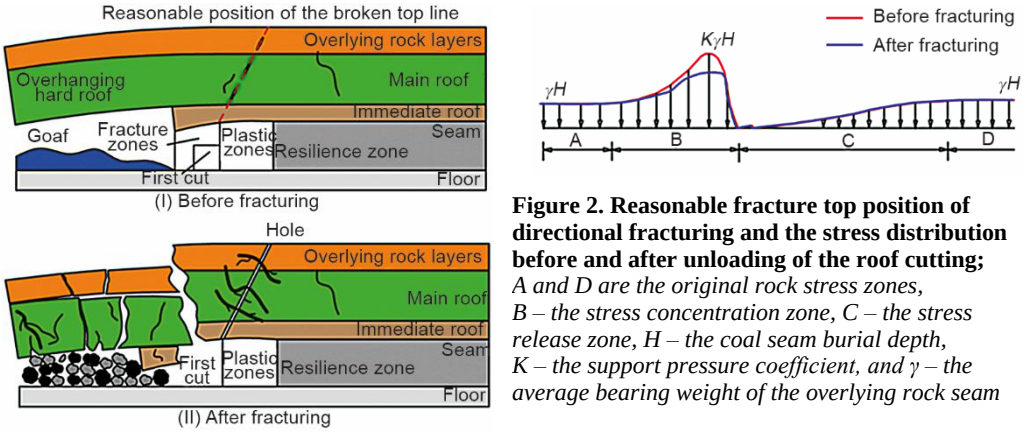

Figure 2. Reasonable fracture top position of directional fracturing and the stress distribution before and after unloading of the roof cutting; *A and D are the original rock stress zones, B – the stress concentration zone, C – the stress release zone, H – the coal seam burial depth, K – the support pressure coefficient, and γ – the average bearing weight of the overlying rock seam*

A 3-D model of hydraulic fracture propagation in the hard roof is shown in fig. 4. We assume that the critical water pressure for hydraulic fracture extension is P_c, and P_1, P_2, and P_3 are the extension pressure of hydraulic fracture in rock formation #1~#3, respectively.

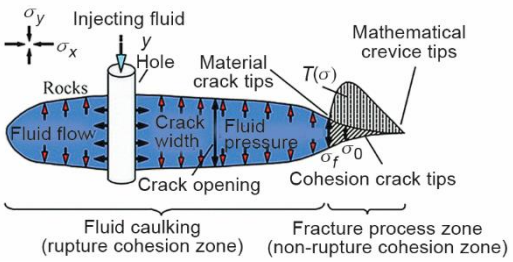

Figure 3. Hydraulic fracture and fracture process zone; *σ_o is the cohesive crack tip damage critical value and σ_f is the material crack tip complete failure critical value*

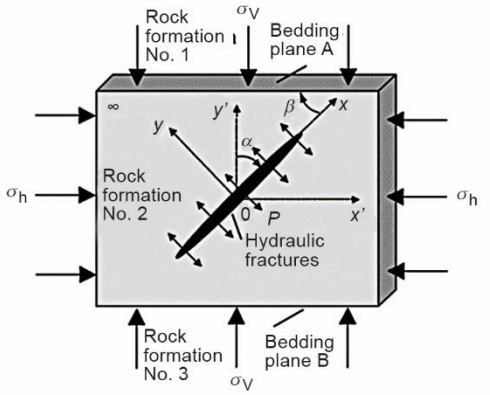

Figure 4. Hydraulic fracturing mechanical model; *σ_V [MPa] is the vertical stress, σ_h [MPa] – the minimum horizontal principal stress, α – the inclination of bedding plane, and β – the intersection angle between the fracture and the bedding plane, $\alpha + \beta = 90°$*

Propagation of hydraulic fracturing at the bedding plane

Fractures within the rock are generally randomly distributed in 3-D. In this paper, the influence of water pressure on fracture mode and the calculation of critical water pressure are studied based on the single fracture shown in fig. 4. The closed fracture shown in fig. 4. is subject to far-field geostress σ_V and σ_h. The water pressure in the fracture is p. Assuming that the water pressure acts equally in all directions along the fracture, the rock is brittle and elastic. The stress state analysis shows that the positive stress σ and the shear stress τ on the crack are, respectively:

$$\sigma = -\left(\frac{\sigma_{\mathrm{V}} + \sigma_{\mathrm{h}}}{2} - \frac{\sigma_{\mathrm{V}} - \sigma_{\mathrm{h}}}{2} \cos 2\beta - p \right) \tag{1}$$

$$\tau = -\frac{\sigma_{\mathrm{V}} - \sigma_{\mathrm{h}}}{2} \sin 2\beta \tag{2}$$

When the normal positive stress on the fracture surface is tensile stress, the fracture extension problem belongs to the I-II tension-shear composite type in fracture mechanics. In this paper, the approximate fracture criterion commonly used in engineering is adopted, I-II tension-shear composite crack instability criterion can be expressed:

$$K_I + K_{II} = K_{I\mathrm{c}} \tag{3}$$

where $K_{I\mathrm{c}}$ is the type I fracture toughness, K_I and K_{II} are type I and type II stress intensity factors, respectively.

$$K_I = \sigma\sqrt{\pi a}, \quad K_{II} = \tau\sqrt{\pi a} \tag{4}$$

where a is the fracture half-length.

To obtain the critical water pressure P_{c}, we substitute eqs. (1) and (2) into (4) and then into (3):

$$P_{\mathrm{c}} = \frac{\sigma_{\mathrm{V}} + \sigma_{\mathrm{h}}}{2} - \frac{\sigma_{\mathrm{V}} - \sigma_{\mathrm{h}}}{2} \cos 2\beta + \left| \frac{\sigma_{\mathrm{V}} - \sigma_{\mathrm{h}}}{2} \sin 2\beta \right| + \frac{K_{I\mathrm{c}}}{\sqrt{\pi a}} \tag{5}$$

From eq. (5), it can be seen that the critical water pressure under certain geostress conditions is related to the fracture direction. Let $m = \sigma_{\mathrm{h}}/\sigma_{\mathrm{V}}$, while defining the generalized critical internal water pressure $P' = (P'_{\mathrm{c}} - K_{I\mathrm{c}}/\sqrt{\pi a})/\sigma_{\mathrm{V}}$ at tension-shear mixed fracturing. The P' can be calculated:

$$P' = \frac{m+1}{2} + \frac{m-1}{2} \cos 2\beta + \left| \frac{m-1}{2} \sin 2\beta \right| \tag{6}$$

Lateral pressure coefficient m reflects the magnitude of the surrounding pressure around the fracture [14]. The fracture instability and direction of extension of rock fractures are directly related to the surrounding pressure. As shown in fig. 5.

Relationship between hydraulic fractures and natural fractures

Gu *et al.* [15] divided the hydraulic fracture-natural fracture interaction into two stages. Cook and Underwood [16] and Zhao and Chen [17] concluded that fractures might undergo extensional behavior at the stratigraphic interface such as propagating through the layers, expansion along the interface, tip extinction. Altammar *et al.* [18] observed that the possible propagation behavior of fractures at the interface includes penetration propagation, new born fractures at the other side of the interface, inflexion propagation, and expansion along the interface. Wu *et al.* [19] concluded through experiments that hydraulic fractures may form penetrating, stop-fracture, and deviated fractures when they reached the coal-rock interface. The process of hydraulic fracture and natural fracture interaction can be described as shown in fig. 6.

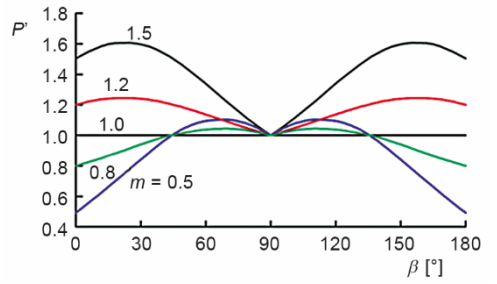

Figure 5. Relationship between generalized critical water pressure and direction of fracture under tension-shear mixed cracking

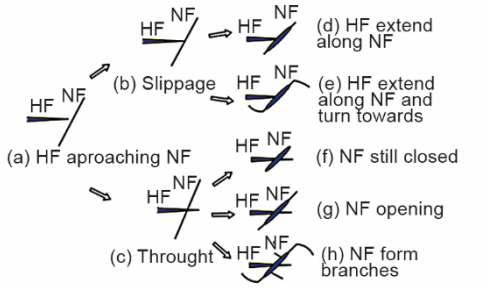

Figure 6. Interaction process between hydraulic fracture and nature fracture

The propagation pressure in a hydraulic fracture along the bedding plane mainly depends on the bedding dip angle, the angle of intersection between the hydraulic fracture and the bedding plane, the geostress and the nature of the bedding plane and other elements [20]. When a hydraulic fracture propagates in rock formation #2 as shown in fig. 4, the propagation pattern may be as follows [21]: when $\min(P_1, P_2, P_3, P_c) = P_c$, after the hydraulic fracture intersects with the bedding plane, the fracture will propagate along the bedding plane *A* and *B*. When $\min(P_1, P_2, P_3, P_c) = P_2$, hydraulic fracture will always propagate in rock formation No. 2, creating a clear occlusion effect. When $\min(P_1, P_2, P_3, P_c) = P_1$, then the hydraulic fracture will pass through the bedding plane *A* and enter the rock formation No. 1. If at this point $\min(P_2, P_3, P_c) = P_3$, the hydraulic fracture will pass through the bedding plane *B* and enter the rock formation No. 2. If $\min(P_2, P_3, P_c) = P_c$, the hydraulic fracture will propagate along the bedding plane *B*. If $\min(P_2, P_3, P_c) = P_2$, the lower part of the hydraulic fracture will be limited to the rock formation No. 2. When $\min(P_1, P_2, P_3, P_c) = P_3$, the hydraulic fracture will pass through the bedding plane *A* and enter the rock formation No. 3. If $\min(P_1, P_2, P_c) = P_1$, the hydraulic fracture will pass through the bedding plane *A* and enter the rock formation No. 1. If $\min(P_1, P_2, P_c) = P_c$, the hydraulic fracture will propagate along the bedding plane *A*. If $\min(P_1, P_2, P_c) = P_2$, the upper part of the hydraulic fracture will be limited to the rock formation No. 2.

Fracturing practice

The fracturing holes were drilled with drills of Ø56 mm diameter. Two types of holes, *S* and *L*, with a hole spacing of 10 m are crossed in the open-off cut. Two types of fracturing holes, *A* and *J*, are arranged in crossheading, and hole *A* is drilled parallel to the roadway toward the goaf orientations. Both holes *A* and *J* have a hole spacing of 10 m. The parameters of each borehole are shown in tab. 1.

Table 1. Parameters of drilling design

Drilling number	Azimuth [°]	Drilling depth [m]	Elevation [°]
S	133	33.0	55
L	133	30.0	45
A	223	26.0	55
J		26.0	55

Each hole is sealed from the bottom of the borehole and in the mode of retreating hydraulic fracturing, with fracturing once every 3 m interval and 3-4 times in each hole.

It can be seen from the experiments that when the incision plane is perpendicular to the bedding plane, the coal stone has the highest fracture toughness, which between 0.3-0.4 MPa $m^{0.5}$ and with an average of 0.364 Mpa $m^{0.5}$. When the incision plane is parallel to the bedding plane, the fracture toughness K_{Ic} of the coal stone has an average of 0.120 Mpa $m^{0.5}$. The compressive strength σ_V of the main roof of the practice mine is approximately 30.5 MPa. The inner friction angle β is about 36°36′. The current depth of the coal seam is about 440 m, the third principal stress is calculated using $\sigma_h = 0.0289H + 2.536$ can be calculated as 15.3 Mpa. Fracture half-length taken as three times the radius of the borehole, which is 84 mm. According to the parameters and fracture toughness K_{Ic} values, based on the equation, P_c can be calculated as 28.5 MPa and 28.7 MPa, respectively, $m = 0.5$, $P' = 0.97$. Through field fracturing practice, the effective initial pressure monitored by pressure sensor on the high-pressure pipeline is 28-30.2 MPa, which coincides with the calculated critical pressure.

Fracturing effect investigation: at 12 m of working face, a large area of the immediate roof of the goaf collapse off and forms a mat. As the stopping progresses, the stent load peaks three times, with the main roof's initial pressure interval dropping from 35 m to 23 m after fracturing. The main roof was gradually collapsed in layers and in stages, and no large area collapse phenomenon.

The results of mineral pressure manifestation were a maximum amount of displacement on both sides of the roadway was 165 mm, and the maximum amount of displacement on the roof and bottom plates was 121 mm. when no hydraulic fracturing was performed. After hydraulic fracturing, both sides of the roadway shifted up to 38 mm, and the top plate of the roadway sank up to 29 mm. The amount of shifting on both sides was obviously reduced, the deformation of the roadway became smaller, and the bottom drum of the adjacent roadway was not obvious.

Discussion and conclusions

The fracture-induced property change was studied in [22], and the fracture patterns and the fracture-induced properties can be described by the fractal dimensions [23-28], the fractal fracture is a research frontier [29] in the future. This paper can obtain the following conclusions:

- The complex fractures after hydraulic fracturing include both nascent hydraulic fractures perpendicular to the bedding plane and extensional extension of hydraulic fractures along the weak bedding plane, forming a fracture network with both longitudinal and transverse fractures. Overall, the direction of hydraulic fracture extension is influenced by the extension pressure in different rock formations and the extension critical pressure.
- The initial rupture water pressure monitored by the directional hydraulic fracturing orifice of the hard roof in the practice mine is 28.0-30.2 MPa. Directional hydraulic fracturing can make the coal seam roof collapse gradually in layers and in stages, effectively reducing the degree of pressure on the roof, and at the same time, the bottom drum of the adjacent roadway is significantly suppressed, indicating that hydraulic fracturing has a better effect of controlling the hard roof.

Acknowledgment

This work was supported by National Natural Science Foundation of China (grant No. 51774116), the training plan of young backbone teachers in Colleges and universities of

Henan Province (grant No. 2019GGJS052), and the Fundamental Research Funds for the Universities of Henan Province (grant No. NSFRF200327).

References

[1] Feng, Y. J., Kang, H. P., Test on Hard and Stable Roof Control by Means of Directional Hydraulic Fracturing in Coal Mine (in Chinese), *Chinese Journal of Rock Mechanics and Engineering*, *31* (2012), 6, pp. 1148-1155
[2] Yu, B., *et al.*, Effect of Hard Roof Breaking on Gas Emission in Fully-Mechanized Sublevel Caving Mining of Extremely Thick Coal Seam (in Chinese), *Journal of China Coal Society*, *43* (2018), 8, pp. 2243-2249
[3] Zhang, T., *et al.*, Modeling of Multiphysical-Chemical Coupling for Coordinated Mining of Coal and Uranium in a Complex Hydrogeological Environment, *Natural Resources Research*, *30* (2020), 1, pp. 571-589
[4] Lin, C., *et al.*, Experiment Simulation of Hydraulic Fracture in Colliery Hard Roof Control, *Journal of Petroleum Science and Engineering*, *138* (2016), Feb., pp. 265-271
[5] Desroches, J., *et al.*, The Crack Tip Region in Hydraulic Fracturing, *Proceedings of the Royal Society A : Mathematical Physical & Engineering Sciences*, *447* (1994), 1929, pp. 39-48
[6] Zhou, J., *et al.*, Analysis of Fracture Propagation Behavior and Fracture Geometry Using a Tri-Axial Fracturing System in Naturally Fractured Reservoirs, *International Journal of Rock Mechanics & Mining Sciences*, *45* (2008), 7, pp. 1143-1152
[7] Kang, H. P., Feng, Y. J., Monitoring of Stress Change in Coal Seam Caused by Directional Hydraulic Fracturing in Working Face with Strong Roof and Its Evolution (in Chinese), *Journal of China Coal Society*, *37* (2012), 12, pp. 1953-1959
[8] Huang, B. X., *et al.*, Theory and Technology of Controlling Hard Roof with Hydraulic Fracturing in Underground Mining (in Chinese), *Chinese Journal of Rock Mechanics and Engineering*, *36* (2017), 12, pp. 2954-2970
[9] Green, A. E., Sneddon, I. N., The Distribution of Stress in the Neighbourhood of a Flat Elliptical Crack in an Elastic Solid, *Mathematical Proceedings of the Cambridge Philosophical Society*, *46* (1950), 1, pp. 159-164
[10] Nordgren, R. P., Propagation of a Vertical Hydraulic Fracture, *Society of Petroleum Engineers Journal*, *12* (1970), 4, pp. 306-314
[11] Banerjee, G., *et al.*, Hard Roof Management-A Key for High Productivity in Longwall Coal Mines, *Journal of Mines, Metals and Fuels*, *51* (2003), 7, pp. 238-244
[12] Wang, H., *et al.*, Numerical Simulation of Granite Hydraulic Fracture Propagation Under the Influence of Natural Fractures (in Chinese), *Acta Geologica Sinica*, *94* (2020), 7, pp. 2124-2130
[13] Chen, Z. R., *et al.*, Cohesive Zone Finite Element-Based Modeling of Hydraulic Fractures, *Acta Mechanica Solida Sinica*, *22* (2009), 5, pp. 443-452
[14] Li, Z. L., *et al.*, Analysis of Hydraulic Fracturing and Calculation of Critical Internal Water Pressure of Rock Fracture (in Chinese), *Rock and Soil Mechanics*, *26* (2005), 8, pp. 1216-1220
[15] Gu, H. R., *et al.*, Hydraulic Fracture Crossing Natural Fracture at Nonorthogonal Angles: A Criterion and Its Validation. *SPE Production & Operations*, *27* (2012), 1, pp. 20-26
[16] Cooke, M. L., Underwood, C.A., Fracture Termination and Step-Over at Bedding Interfaces Due to Frictional Slip and Interface Opening, *Journal of Structural Geology*, *23* (2001), 2, pp. 223-238
[17] Zhao, H. F., Chen, M., Extending Behavior of Hydraulic Fracture when Reaching Formation Interface, *Journal of Petroleum Science and Engineering*, *74* (2010), 1-2, pp. 26-30
[18] Altammar, M. J., *et al.*, Effect of Geological Layer Properties on Hydraulic Fracture Initiation and Propagation: An Experimental Study, *SPE Journal*, *24* (2019), 2, pp. 757-794
[19] Wu, P. F., *et al.*, Mechanism and Experimental Investigation of the Formation of Hydro-Fracture System by Fracturing Through the Interface of Large-Size Coal-Rock, (in Chinese), *Journal of China Coal Society*, *43* (2018), 5, pp. 1381-1389
[20] Wu, Y. Z., Yang, J. W., True Tri-Axial Directional Hydraulic Fracturing Test on Sandstone with Transverse Grooves in Coal Mine, (in Chinese), *Journal of China Coal Society*, *45* (2020), 3, pp. 927-935
[21] Patutin, A., Serdyukov, S., Transverse Hydraulic Fracture Initiation by Indentation in an Uncased Borehole, *Procedia Engineering*, *191* (2017), Dec., pp. 287-290

[22] Cao, H., *et al.*, A Fracture-Induced Adhesive Wear Criterion and Its Application to the Simulation of Wear Process of the Point Contacts Under Mixed Lubrication Condition, *Facta Universitatis Series Mechanical Engineering, 19* (2021), 1, pp. 23-38
[23] He, C. H., *et al.*, A Fractal Model for the Internal Temperature Response of a Porous Concrete, *Applied and Computational Mathematics, 21* (2022), 1, pp. 71-77
[24] He, C. H., *et al.*, A Novel Bond Stress-Slip Model for 3-D Printed Concretes, *Discrete and Continuous Dynamical Systems-Series S, 15* (2022), 7, pp. 1669-1683
[25] Zuo, Y. T., Liu, H. J., Fractal Approach to Mechanical and Electrical Properties of Graphene/Sic Composites, *Facta Universitatis-Series Mechanical Engineering, 19* (2021), 2, pp. 271-284
[26] He, J. H., *et al.*, Forced Non-Linear Oscillator in a Fractal Space, *Facta Universitatis Series Mechanical Engineering, 20* (2022), 1, 2022, pp. 1-20
[27] He, J. H., Qian, M. Y., A Fractal Approach to the Diffusion Process of Red Ink in a Saline Water, *Thermal Science*, *26* (2022), 3B, pp. 2447-2451
[28] Qian, M. Y., He, J. H., Two-Scale Thermal Science for Modern Life –Making the Impossible Possible, *Thermal Science*, *26* (2022), 3B, pp. 2409-2412
[29] Moein, M. J. A., *et al.*, Fractal Characteristics of Fractures in Crystalline Basement Rocks: Insights from Depth-Dependent Correlation Analyses to 5 km Depth, *International Journal of Rock Mechanics and Mining Sciences*, *155* (2022), Jun., 105138

Paper submitted: December 12, 2021
Paper revised: June 30, 2022
Paper accepted: June 30, 2022

© 2023 Society of Thermal Engineers of Serbia.
Published by the Vinča Institute of Nuclear Sciences, Belgrade, Serbia.
This is an open access article distributed under the CC BY-NC-ND 4.0 terms and conditions.